Journal of Sound and Vibration (2002) **249**(5), 955–970
doi:10.1006/jsvi.2001.3917, available online at http://www.idealibrary.com on IDEAL®

EXTRACTION OF STRUCTURAL SYSTEM MATRICES FROM AN IDENTIFIED STATE-SPACE SYSTEM USING THE COMBINED MEASUREMENTS OF DVA

W. J. Ko and C. F. Hung

Department of Naval Architecture and Ocean Engineering, National Taiwan University, 73 Chow-Shan Road, Taipei, Taiwan, Republic of China.
E-mail: hungef@ccms.ntu.edu.tw

(*Received* 20 *January* 2001, *and in final form* 10 *July* 2001)

A time domain method for the extraction of the structural system matrices (mass, damping and stiffness matrices) from an identified state-space system is proposed in this paper using the combined measurements of displacement, velocity and acceleration (DVA) together with the input excitations. The method is based on the invariance of continuous-time Markov parameters. An explicit expression of the relationship between the continuous-time Markov parameters, the structural system matrices, and the influence matrices for output DVA as well as the input force has been derived. The determination of structural system matrices is also valid when only the displacement, velocity or acceleration responses are measured. In this paper, the equivalent state system matrices are obtained by an algorithm, which combines the eigensystem realization algorithm (ERA) and the autoregressive with exogeneous (ARX) model. The ARX model provides the necessary discrete-time Markov parameters from the measured input and output data, and then the equivalent state system matrices are identified from discrete-time Markov parameters by using the ERA. A lumped mass model with three degrees of freedom is employed to illustrate the accuracy and feasibility of the presented method.

1. INTRODUCTION

The development of accurate mathematical models for the identification of the dynamic characteristics of complex structures is a topic with broad-ranging applications. Examples of applications include naval architecture, ocean engineering, aircraft spacecraft, mechanical, and civil engineering structures. The most popular approaches in the field of structural system identification are the physical and modal models. The modal model defines the dynamic behaviors of structures in terms of natural frequencies, damping ratios and mode shapes. Applications of modal model for updating an analysis model or for detecting structural damage have been studied in various engineering fields [1–7]. The physical model, also called spatial model [8], is characterized by the structural system matrices (**M**, **E**, **K**), which are the mass, damping and stiffness matrices respectively. Because the mode shapes are not uniquely defined, Baruch [9] showed that even full modal data are insufficient for the identification of both mass and stiffness matrices. The modal model estimated from vibration responses with unknown input force, cannot be transformed directly into the physical model.

In recent years, various methods for the identification of structural system matrices have been developed. Chen *et al.* [10, 11] presented a frequency-domain method to estimate the

0022-460X/02/050955 + 16 $35.00/0

system matrices of structure directly from receptance FRFs, which were estimated from displacement response. Alvin *et al.* [12] and Yuan *et al.* [13] determined mass and stiffness matrices from modal test data. The methods used in these papers were based on the normal modal data, and the damping matrix was not evaluated. Okuma *et al.* [14] developed spatial matrices from complex modal data, which were estimated from accelerance FRFs. Juang and Pappa [15, 16] developed the eigensystem realization algorithm (ERA) to estimate the natural frequencies and damping ratios of a dynamic system from the known Markov parameters. Yang and Yeh [17] employed the ERA to identify the system matrices of a vibrating structure from the displacement-based Markov parameters, which were estimated from measured displacement responses together with the excitation forces. Chaudhary *et al.* [18] proposed a two-step method, the former is the estimation of complex modal parameters using system realization theory from seismic records, and the latter is the identification of structural parameters from the estimated complex modes for identifying the physical model of two base-isolated bridges. In the aforementioned papers, only a single type of sensor was used, the combined measurement of displacement, velocity and acceleration (DVA) has not been found. In some modal testing circumstance, different types of sensors may be used for the identification of structural models. Hung *et al.* [19] developed a transformation method for extracting the modal parameters from the combined measurements of DVA under unknown input force. In this paper, a time domain method for the extraction of mass, damping and stiffness matrices from an identified continuous-time state-space system has been developed using the combined measurements of DVA together with the input excitation. An explicit expression based on the invariant principle of continuous-time Markov parameters using the combined DVA data for determining the structural system matrices has been derived. In this paper, the ERA method developed by Juang and Pappa [15, 16, 20] is employed to obtain an equivalent state-space system. Because the Markov parameters used in the ERA method cannot be measured directly in a vibration test, an autoregressive with exogeneous (ARX) model is used in this paper to obtain the necessary Markov parameters from the combined DVA output response data together with the input forces.

2. STATE-SPACE REPRESENTATION OF STRUCTURAL SYSTEM

The equations of motion for a linear-elastic structure with n degrees of freedom (d.o.f.) can be expressed in matrix form as

$$\mathbf{M}\ddot{x}(t) + \mathbf{E}\dot{x}(t) + \mathbf{K}x(t) = \mathbf{B}_0 u(t), \tag{1}$$

where t is the continuous time, $x(t) \in R^{n\times 1}$ is the displacement vector, $u(t) \in R^{r\times 1}$ is the excitation force vector, $\mathbf{B}_0 \in R^{n\times r}$ is the input influence matrix describing the measure locations of excitation forces vector, $\mathbf{M} \in R^{n\times n}$ is the positive-definite mass matrix, $\mathbf{E} \in R^{n\times n}$ is the positive semi-definite damping matrix, and $\mathbf{K} \in R^{n\times n}$ is the positive semi-definite stiffness matrix. The dot indicates differentiation with respect to time. In the practical experimental identification of dynamic characteristics of structures, not all of the degrees of freedom are observed. Therefore, there exists a measurement system with l sensors under a prescribed arrangement for measuring the dynamic response of structures. If the sensors of displacement, velocity, and acceleration are arranged on different locations to measure the dynamic responses simultaneously, then the combined output equation of the structural system for DVA measurements can be written as [20]

$$y(t) = \mathbf{C}_d x(t) + \mathbf{C}_v \dot{x}(t) + \mathbf{C}_a \ddot{x}(t), \tag{2}$$

where $\mathbf{C}_d, \mathbf{C}_v, \mathbf{C}_a \in R^{l\times n}$ are the output influence matrices for the vectors of displacement, velocity and acceleration respectively. After introducing a state vector, $z(t) = \{x(t); \dot{x}(t)\} \in R^{2n\times 1}$, the equations of motion for the physical model described by equation (1) can be transformed into the following state equation of motion:

$$\dot{z}(t) = \mathbf{A}_c z(t) + \mathbf{B}_c u(t), \tag{3}$$

where $\mathbf{A}_c \in R^{2n\times 2n}$ is the system matrix, $\mathbf{B}_c \in R^{2n\times r}$ is the input matrix, and

$$\mathbf{A}_c = \begin{bmatrix} 0 & \mathbf{I} \\ -\mathbf{M}^{-1}\mathbf{K} & -\mathbf{M}^{-1}\mathbf{E} \end{bmatrix}, \qquad \mathbf{B}_c = \begin{bmatrix} 0 \\ \mathbf{M}^{-1}\mathbf{B}_0 \end{bmatrix}. \tag{4a,b}$$

Using the same definition of state vector, the output equation in equation (2) can be transformed as

$$y(t) = \mathbf{C}z(t) + \mathbf{D}u(t), \tag{5}$$

where

$$\mathbf{C} = [\mathbf{C}_d - \mathbf{C}_a\mathbf{M}^{-1}\mathbf{K} \quad \mathbf{C}_v - \mathbf{C}_a\mathbf{M}^{-1}\mathbf{E}], \qquad \mathbf{D} = \mathbf{C}_a\mathbf{M}^{-1}\mathbf{B}_0, \tag{6a,b}$$

where $\mathbf{C} \in R^{l\times 2n}$ is the output influence matrix for the state vector $z(t)$, $\mathbf{D} \in R^{l\times r}$ is the direct transmission matrix. The matrix $\mathbf{D}$ will disappear from equation (5) when accelerometers are not used for output measurements. Equations (3) and (5) constitute a continuous-time multiple input and multiple output (MIMO) state-space model for a finite-dimensional dynamic system. For convenience, a quadruplet, namely $(\mathbf{A}_c, \mathbf{B}_c, \mathbf{C}, \mathbf{D})$, stands for the continuous-time physical state model to be used in this paper. The output responses of equation (5) with non-zero initial conditions can be expressed in the following form [21]:

$$y(t) = \mathbf{C}e^{\mathbf{A}_c(t-t_0)}z(t_0) + \int_0^t \mathbf{h}(t-\tau)u(\tau)\,\mathrm{d}\tau, \tag{7}$$

where $z(t_0)$ is the state vector at initial time t_0, $\mathbf{h}(t) = \mathbf{C}e^{\mathbf{A}_c t}\mathbf{B}_c + \mathbf{D}\delta(t)$ is the impulse response function (IRF), and $\delta(t)$ is the Dirac delta function. The IRF characterizes the dynamics of a structural system in the time domain and is independent of the output responses and the excitation forces for a linear-elastic structural system. The IRF can be expanded by power series as [21]

$$\begin{aligned} \mathbf{h}(t) &= \mathbf{C}e^{\mathbf{A}_c t}\mathbf{B}_c + \mathbf{D}\delta(t) \\ &= \sum_{k=1}^{\infty} \frac{\mathbf{h}_k}{(k-1)!} t^{k-1} + \mathbf{h}_0\delta(t), \end{aligned} \tag{8}$$

where

$$\mathbf{h}_k = \begin{cases} \mathbf{D}, & k = 0, \\ \mathbf{C}\mathbf{A}_c^{k-1}\mathbf{B}_c, & k \geqslant 1, \end{cases} \tag{9}$$

where $\mathbf{h}_k \in R^{l\times r}$ is the kth coefficient matrix of the power-series expansion of the IRF. The collection of all these coefficient matrices, i.e., $\mathbf{h} = \{\mathbf{h}_0, \mathbf{h}_1, \mathbf{h}_2, \ldots\}$, is called the continuous-time Markov parameters sequence [21]. Although the column and row dimensions of the IRF for an experiment depend upon the number of output measurements and input excitations, the type and magnitude of IRF depend on the structural system characteristics, i.e., the mass, damping and stiffness properties.

3. EQUIVALENT DISCRETE-TIME STATE-SPACE MODEL

A discrete-time state-space system related to the continuous-time system can be obtained through sampling and zero-order-hold procedure with sampling time Δt. The discrete-time state equation and output equation can be written as

$$z_{k+1} = \mathbf{A}_d z_k + \mathbf{B}_d u_k, \qquad y_k = \mathbf{C} z_k + \mathbf{D} u_k \tag{10, 11}$$

and

$$\mathbf{A}_d = \mathrm{e}^{\mathbf{A}_c \Delta t}, \qquad \mathbf{B}_d = (\mathbf{A}_d - I)\mathbf{A}_c^{-1}\mathbf{B}_c, \tag{12a,b}$$

where k is the integer discrete-time index at time instant $t = k\Delta t$, z_k is the state vector $z(t)$ at the discrete time k, u_k is the force vector, y_k is the output vector $\mathbf{A}_d$ is the discrete state system matrix, and $\mathbf{B}_d$ is the discrete input influence matrix for the state vector z_k. The output matrix $\mathbf{C}$ and the direct transmission matrix $\mathbf{D}$ are unchanged during the zero-order-hold operations [20]. The dimensions of the discrete system are equal to those of the continuous system. A quadruplet written as ($\mathbf{A}_d$, $\mathbf{B}_d$, $\mathbf{C}$, $\mathbf{D}$) in discrete time can also be used to describe equations (10) and (11) for convenience. The discrete-time Markov parameters can also be defined in the same way as in continuous time

$$\mathbf{g}_k = \begin{cases} \mathbf{D}, & k = 0, \\ \mathbf{C}\mathbf{A}_d^{k-1}\mathbf{B}_d, & k \geqslant 1. \end{cases} \tag{13}$$

The identified discrete-time quadruplet ($\bar{\mathbf{A}}_d$, $\bar{\mathbf{B}}_d$, $\bar{\mathbf{C}}$, $\bar{\mathbf{D}}$) can be estimated from the measured output responses and excitation forces by various approaches. Here, the variables with superscript "bar" indicate the identified properties from measured data.

We employ the ERA method to determine the discrete-time state-space system from the estimated Markov parameters. The Markov parameters can be estimated by various approaches. It is determined from an ARX model in this paper. In order to obtain accurate vibration modes, the size of the state vector is over-specified generally. Actually, the over-specified discrete-time state-space system is employed for fitting a set of measured output responses and input excitations in practical cases.

The identified continuous quadruplet ($\bar{\mathbf{A}}_c$, $\bar{\mathbf{B}}_c$, $\bar{\mathbf{C}}$, $\bar{\mathbf{D}}$) that has the same size as the physical model, can be estimated from the identified discrete-time quadruplet ($\bar{\mathbf{A}}_d$, $\bar{\mathbf{B}}_d$, $\bar{\mathbf{C}}$, $\bar{\mathbf{D}}$) by the inverse computation of equations (12a) and (12b)

$$\bar{\mathbf{A}}_c < \ln(\bar{\mathbf{A}}_d)/\Delta t, \qquad \bar{\mathbf{B}}_c = \bar{\mathbf{A}}_c(\bar{\mathbf{A}}_d - I)^{-1}\bar{\mathbf{B}}_d. \tag{14a,b}$$

The contents of the identified quadruplet ($\bar{\mathbf{A}}_c$, $\bar{\mathbf{B}}_c$, $\bar{\mathbf{C}}$, $\bar{\mathbf{D}}$) are generally not the same as the physical quadruplet ($\mathbf{A}_c$, $\mathbf{B}_c$, $\mathbf{C}$, $\mathbf{D}$). If the state-space system is estimated from measured data by an accurate and effective method, the identified quadruplet is equivalent to the physical model from the viewpoint of the continuous-time Markov parameters.

The ARX model with q-order, l-output and r-input to simulate an MIMO linear time-invariant system can be written as

$$y_k + \sum_{i=1}^{q} \mathbf{a}_i y_{k-i} = \mathbf{b}_0 u_k + \sum_{i=1}^{q} \mathbf{b}_i u_{k-i} + \varepsilon_k, \tag{15}$$

where $\mathbf{a}_i \in R^{l\times 1}$ and $\mathbf{b}_i \in R^{l\times r}$ are the AR and X coefficient matrices, respectively; $\varepsilon_k \in R^{l\times l}$ is an error vector which simulates the model errors and measurement errors. The coefficient matrices of the ARX model can be estimated by the prediction error method [22, 23]. After the ARX model is identified from the measured DVA output responses and the input

excitations, the estimation of Markov parameters, $\bar{\mathbf{g}}_i \in R^{l\times r}$, in discrete time can be computed through [24]

$$\bar{\mathbf{g}}_0 = \bar{\mathbf{b}}_0, \qquad \bar{\mathbf{g}}_i = \bar{\mathbf{b}}_i - \sum_{j=1}^{i} \bar{\mathbf{a}}_j \bar{\mathbf{g}}_{i-j}, \quad i = 1, 2, \ldots, p, \tag{16a,b}$$

$$\bar{\mathbf{g}}_i = -\sum_{j=1}^{i} \bar{\mathbf{a}}_j \bar{\mathbf{g}}_{i-j}, \qquad i = p+1, p+2, \ldots, \infty. \tag{61c}$$

The order of the ARX model selected should be high enough to estimate the accurate Markov parameters. The dynamic system described by equations (10) and (11) can be identified using the ERA with the Markov parameters in equations (16a)–(16c).

The procedure for obtaining the Markov parameters using an ARX model is actually an observer Kalman filter identification (OKID) presented in references [25, 26]. In this paper, the discrete-time Markov parameters are computed directly from the ARX model, and the computation of observer's gain is not needed. In the ERA, we use the discrete-time Markov parameters to construct a generalized block Hankel matrix, $\mathbf{G}(i-1) \in R^{\alpha l\times \beta r}$

$$\mathbf{G}(i-1) = \begin{bmatrix} \mathbf{g}_i & \mathbf{g}_{i+1} & \cdots & \mathbf{g}_{i+\beta-1} \\ \mathbf{g}_{i+1} & \mathbf{g}_{i+2} & \cdots & \mathbf{g}_{i+\beta} \\ \vdots & \vdots & \ddots & \vdots \\ \mathbf{g}_{i+\alpha-1} & \mathbf{g}_{i+\alpha} & \cdots & \mathbf{g}_{i+\alpha+\beta-2} \end{bmatrix} = \mathbf{C}_\alpha \mathbf{A}_d^{i-1} \mathbf{O}_\beta, \tag{17}$$

where

$$\mathbf{C}_\alpha = \begin{bmatrix} \mathbf{C} \\ \mathbf{C}\mathbf{A}_d \\ \mathbf{C}\mathbf{A}_d^2 \\ \vdots \\ \mathbf{C}\mathbf{A}_d^{\alpha-1} \end{bmatrix}, \tag{18}$$

$$\mathbf{O}_\beta = [\mathbf{B}_d \quad \mathbf{A}_d\mathbf{B}_d \quad \mathbf{A}_d\mathbf{B}_d^2 \quad \cdots \quad \mathbf{A}_d\mathbf{B}_d^{\beta-1}], \tag{19}$$

where α and β are integers; $\mathbf{O}_\beta \in R^{l\alpha\times 2n}$ is the observability matrix, and $\mathbf{C}_\beta \in R^{2n\times \beta r}$ is the controllability matrix. The ERA uses the singular value decomposition of matrix $\mathbf{G}(0)$

$$\mathbf{G}(0) = \mathbf{C}_\alpha \mathbf{O}_\beta = \mathbf{U}\mathbf{S}\mathbf{V}^{\mathrm{T}} = [\mathbf{U}_1 \quad \mathbf{U}_2] \begin{bmatrix} \mathbf{S}_1 & 0 \\ 0 & 0 \end{bmatrix} \begin{bmatrix} \mathbf{V}_1^{\mathrm{T}} \\ \mathbf{V}_2^{\mathrm{T}} \end{bmatrix}, \tag{20}$$

where $\mathbf{U} \in R^{l\alpha\times l\alpha}$ and $\mathbf{V} \in R^{\beta r\times \beta r}$ are orthogonal matrices; $\mathbf{S} \in R^{\alpha l\times \beta r}$ is a matrix comprising all singular values of $\mathbf{G}(0)$, $\mathbf{S}_1$ is a non-singular diagonal matrix that contains all non-zero singular values of $\mathbf{G}(0)$. The rank of $\mathbf{G}(0)$ is actually defined by the number of non-zero singular values. $\mathbf{U}_1$ and $\mathbf{V}_1$ are the left partition of $\mathbf{U}$ and $\mathbf{V}$, respectively, with respect to the non-zero singular value. A minimal realization model, which picks up all non-zero singular values, can be obtained by the ERA to estimate the observability and controllability matrices. The input/output data collected from real world are actually contaminated by measurement noise, and all singular values may be non-zero. A gap in the logarithmic

singular value plot may be used to determine the number of dominant singular values. Equation (20), therefore, can be approximated by balanced realization as

$$\mathbf{G}(0) = \mathbf{C}_\alpha \mathbf{O}_\beta = \mathbf{U}\mathbf{S}\mathbf{V}^{\mathrm{T}} \cong \mathbf{U}_1 \mathbf{S}_1 \mathbf{V}_1^{\mathrm{T}} \cong (\mathbf{U}_1 \mathbf{S}_1^{1/2})(\mathbf{S}_1^{1/2} \mathbf{V}_1^{\mathrm{T}}). \tag{21}$$

The estimation of the observability and controllability matrices in the balanced realization is

$$\bar{\mathbf{C}}_\alpha = \mathbf{U}_1 \mathbf{S}_1^{1/2}, \qquad \bar{\mathbf{O}}_\beta = \mathbf{S}_1^{1/2} \mathbf{V}_1^{\mathrm{T}}. \tag{22a,b}$$

On the basis of the balanced realization, matrix $\mathbf{G}(1)$ can be written as

$$\mathbf{G}(1) = \bar{\mathbf{C}}_\alpha \bar{\mathbf{A}}_d \bar{\mathbf{O}}_\beta = \mathbf{U}_1 \mathbf{S}_1^{1/2} \bar{\mathbf{A}}_d \mathbf{S}_1^{1/2} \mathbf{V}_1^{\mathrm{T}}. \tag{23}$$

The discrete-time state system matrix is now computed through

$$\bar{\mathbf{A}}_d = \mathbf{S}_1^{-1/2} \mathbf{U}_1^{\mathrm{T}} \mathbf{G}(1) \mathbf{V}_1 \mathbf{S}_1^{-1/2}. \tag{24}$$

Using the definition of $\mathbf{E}_l^{\mathrm{T}} = [I_l, 0_l, \ldots, 0_l]$ and $\mathbf{E}_r^{\mathrm{T}} = [I_r, 0_r, \ldots, 0_r]$, the estimation of discrete-time input and output influence matrices are

$$\bar{\mathbf{B}}_d = \mathbf{S}_1^{1/2} \mathbf{V}_1^{\mathrm{T}} \mathbf{E}_r, \qquad \bar{\mathbf{C}} = \mathbf{E}_l^{\mathrm{T}} \mathbf{U}_1 \mathbf{S}_1^{1/2}. \tag{25, 26}$$

Finally, the direct transmission matrix is estimated by the first Markov parameter, i.e.,

$$\bar{\mathbf{D}} = \bar{\mathbf{g}}_0. \tag{27}$$

Once the discrete quadruplet ($\bar{\mathbf{A}}_d$, $\bar{\mathbf{B}}_d$, $\bar{\mathbf{C}}$, $\bar{\mathbf{D}}$) has been identified, the continuous quadruplet ($\bar{\mathbf{A}}_c$, $\bar{\mathbf{B}}_c$, $\bar{\mathbf{C}}$, $\bar{\mathbf{D}}$) can be computed by making use of the zero-order-hold transformation of equation (14).

4. EXTRACTION OF STRUCTURAL SYSTEM MATRICES

Because the continuous-time Markov parameters contain the dynamic characteristics of a linear system, they are also invariant with the change of state vector. Although the continuous-time Markov parameters can be constructed from the continuous quadruplet, their relations to structural system matrices, input influence matrix and output influence matrix for displacement, velocity and acceleration in the case of combined DVA measurements are still not distinct. In this section, we combine the ideas described in sections 2 and 3 to develop a method that extracts the structural system matrices using the invariant characteristic of Markov parameters. The continuous-time Markov parameters can be reconstructed from the identified quadruplet as follows:

$$\bar{\mathbf{h}}_k = \begin{cases} \bar{\mathbf{D}}, & k = 0, \\ \bar{\mathbf{C}} \bar{\mathbf{A}}_c^{k-1} \bar{\mathbf{B}}_c, & k \geqslant 1. \end{cases} \tag{28}$$

If the identified quadruplet has enough accuracy, then the reconstructed Markov parameters will be equivalent to the theoretical one, i.e., $\bar{\mathbf{h}} \cong \mathbf{h}_k$. Following the invariant characteristic of Markov parameters, the relationship between the theoretical and identified Markov parameters can be written as follows:

$$\mathbf{h}_0 = \mathbf{D} = \bar{\mathbf{h}}_0 = \bar{\mathbf{D}}, \qquad \mathbf{h}_k = \mathbf{C}\mathbf{A}_c^{k-1}\mathbf{B}_c = \bar{\mathbf{h}}_k = \bar{\mathbf{C}}\bar{\mathbf{A}}_c^{k-1}\bar{\mathbf{B}}_c, \; k \geqslant 1. \tag{29a,b}$$

From equations (4) and (6), the Markov parameters can be represented as

$$\bar{\mathbf{h}}_0 = \mathbf{D} = \mathbf{C}_a\mathbf{M}^{-1}\mathbf{B}_0, \tag{30a}$$

$$\bar{\mathbf{h}}_1 = \mathbf{CB} = \mathbf{C}_v\mathbf{M}^{-1}\mathbf{B}_0 - \mathbf{C}_a\mathbf{M}^{-1}\mathbf{E}\mathbf{M}^{-1}\mathbf{B}_0, \tag{30b}$$

$$\bar{\mathbf{h}}_2 = \mathbf{CAB} = \mathbf{C}_d\mathbf{M}^{-1}\mathbf{B}_0 - \mathbf{C}_v\mathbf{M}^{-1}\mathbf{E}\mathbf{M}^{-1}\mathbf{B}_0 + \mathbf{C}_a\mathbf{M}^{-1}(\mathbf{E}\mathbf{M}^{-1}\mathbf{E} - \mathbf{K})\mathbf{M}^{-1}\mathbf{B}_0, \tag{30c}$$

$$\bar{\mathbf{h}}_3 = \mathbf{CA}^2\mathbf{B} = -\mathbf{C}_d\mathbf{M}^{-1}\mathbf{E}\mathbf{M}^{-1}\mathbf{B}_0 + \mathbf{C}_v\mathbf{M}^{-1}(\mathbf{E}\mathbf{M}^{-1}\mathbf{E} - \mathbf{K})\mathbf{M}^{-1}\mathbf{B}_0 + \mathbf{C}_a\mathbf{M}^{-1}(\mathbf{K}\mathbf{M}^{-1}\mathbf{E} - \mathbf{E}\mathbf{M}^{-1}\mathbf{E}\mathbf{M}^{-1}\mathbf{E} + \mathbf{E}\mathbf{M}^{-1}\mathbf{K})\mathbf{M}^{-1}\mathbf{B}_0, \tag{30d}$$

$$\begin{aligned}\bar{\mathbf{h}}_4 = \mathbf{CA}^3\mathbf{B} &= \mathbf{C}_d\mathbf{M}^{-1}(\mathbf{E}\mathbf{M}^{-1}\mathbf{E} - \mathbf{K})\mathbf{M}^{-1}\mathbf{B}_0 \\ &\quad + \mathbf{C}_v\mathbf{M}^{-1}(\mathbf{E}\mathbf{M}^{-1}\mathbf{K} + \mathbf{K}\mathbf{M}^{-1}\mathbf{E} - \mathbf{E}\mathbf{M}^{-1}\mathbf{E}\mathbf{M}^{-1}\mathbf{E})\mathbf{M}^{-1}\mathbf{B}_0 \\ &\quad + \mathbf{C}_a\mathbf{M}^{-1}(\mathbf{K}\mathbf{M}^{-1}\mathbf{K} - \mathbf{K}\mathbf{M}^{-1}\mathbf{E}\mathbf{M}^{-1}\mathbf{E} - \mathbf{E}\mathbf{M}^{-1}\mathbf{E}\mathbf{M}^{-1}\mathbf{K} \\ &\quad - \mathbf{E}\mathbf{M}^{-1}\mathbf{K}\mathbf{M}^{-1}\mathbf{E} + \mathbf{E}\mathbf{M}^{-1}\mathbf{E}\mathbf{M}^{-1}\mathbf{E}\mathbf{M}^{-1}\mathbf{E})\mathbf{M}^{-1}\mathbf{B}_0 \\ &\quad \vdots\end{aligned} \tag{30e}$$

The relationship between the Markov parameters, structural system matrices ($\mathbf{M}$, $\mathbf{E}$, $\mathbf{K}$), output influence matrices ($\mathbf{C}_d$, $\mathbf{C}_v$, $\mathbf{C}_a$), and the input influence matrix $\mathbf{B}_0$ is too complicated for the solution of the structural system matrices. The identified Markov parameters are not square matrices when the number of inputs do not have the same number as outputs. The structural system matrices cannot be solved by equation (30) when the identified Markov parameters are not square matrices. In order to solve structural system matrices using the above equations, we assumed temporarily that the number of inputs is equal to the number of outputs, i.e., the input influence matrix $\mathbf{B}_0$ is an identity matrix. Although it is assumed that $\mathbf{B}_0$ is an identity matrix, the above equations, after post-multiplying the inverse of mass matrix, can be rewritten as

$$\bar{\mathbf{h}}_0\mathbf{M} = \mathbf{C}_a, \qquad \bar{\mathbf{h}}_1\mathbf{M} = \mathbf{C}_v - \mathbf{C}_a\mathbf{M}^{-1}\mathbf{E}, \qquad \bar{\mathbf{h}}_2\mathbf{M} = \mathbf{C}_d - \mathbf{C}_v\mathbf{M}^{-1}\mathbf{E} + \mathbf{C}_a\mathbf{M}^{-1}(\mathbf{E}\mathbf{M}^{-1}\mathbf{E} - \mathbf{K}), \tag{31a–c}$$

$$\bar{\mathbf{h}}_3\mathbf{M} = -\mathbf{C}_d\mathbf{M}^{-1}\mathbf{E} + \mathbf{C}_v\mathbf{M}^{-1}(\mathbf{E}\mathbf{M}^{-1}\mathbf{E} - \mathbf{K}) + \mathbf{C}_a\mathbf{M}^{-1}(\mathbf{K}\mathbf{M}^{-1}\mathbf{E} - \mathbf{E}\mathbf{M}^{-1}\mathbf{E}\mathbf{M}^{-1}\mathbf{E} + \mathbf{E}\mathbf{M}^{-1}\mathbf{K}), \tag{31d}$$

$$\begin{aligned}\bar{\mathbf{h}}_4\mathbf{M} &= \mathbf{C}_d\mathbf{M}^{-1}(\mathbf{E}\mathbf{M}^{-1}\mathbf{E} - \mathbf{K}) + \mathbf{C}_v\mathbf{M}^{-1}(\mathbf{E}\mathbf{M}^{-1}\mathbf{K} + \mathbf{K}\mathbf{M}^{-1}\mathbf{E} - \mathbf{E}\mathbf{M}^{-1}\mathbf{E}\mathbf{M}^{-1}\mathbf{E}) \\ &\quad + \mathbf{C}_a\mathbf{M}^{-1}(\mathbf{K}\mathbf{M}^{-1}\mathbf{K} - \mathbf{K}\mathbf{M}^{-1}\mathbf{E}\mathbf{M}^{-1}\mathbf{E} - \mathbf{E}\mathbf{M}^{-1}\mathbf{E}\mathbf{M}^{-1}\mathbf{K} \\ &\quad - \mathbf{E}\mathbf{M}^{-1}\mathbf{K}\mathbf{M}^{-1}\mathbf{E} + \mathbf{E}\mathbf{M}^{-1}\mathbf{E}\mathbf{M}^{-1}\mathbf{E}\mathbf{M}^{-1}\mathbf{E}) \\ &\quad \vdots\end{aligned} \tag{31e}$$

The matrix $\bar{\mathbf{h}}_0$ in equation (31a) is non-singular in the case where only the acceleration signals are measured. In the case of mixed measurements, or where only the displacement or velocity signals is measured, the matrix $\bar{\mathbf{h}}_0$ is generally rank deficient, and the inverse operation of $\bar{\mathbf{h}}_0$ is not available to solve the mass matrix. The output influence matrix for acceleration, $\mathbf{C}_a$, will be the product of $\bar{\mathbf{h}}_0$ and $\mathbf{M}$, and $\mathbf{B}_0$ is essentially an identity matrix. On substituting $\mathbf{C}_a$ into equation (31b), we have

$$\bar{\mathbf{h}}_1\mathbf{M} + \bar{\mathbf{h}}_0\mathbf{E} = \mathbf{C}_v. \tag{32}$$

Equations (31a) and (32) clearly show the relationship of the output influence matrices for acceleration and velocity to the structural system matrices and the two lowest Markov parameters. The relations play a very important role in posterior derivation for solving these complicated equations. On substituting $\mathbf{C}_a = \bar{\mathbf{h}}_0\mathbf{M}$ and $\mathbf{C}_v = \bar{\mathbf{h}}_1\mathbf{M} + \bar{\mathbf{h}}_0\mathbf{E}$ into equation (31c), we obtain

$$\bar{\mathbf{h}}_2\mathbf{M} + \bar{\mathbf{h}}_1\mathbf{E} + \bar{\mathbf{h}}_0\mathbf{K} = \mathbf{C}_d. \tag{33}$$

The structural system matrices seem to be solved externally by casting the set of equations (31a), (32) and (33) into a linear matrix equation. In fact, the direct transmission matrix, $\mathbf{D} = \mathbf{h}_0 = \mathbf{C}_a\mathbf{M}^{-1}$, is actually either a zero matrix or a rank deficient matrix depending on which types of sensors are used in the case of mixed measurements. Therefore, the linear matrix equation cannot be solved exactly by common inverse operation. Hence, we can resort to solving an over-determined linear matrix equations by the following derivations. By substituting the expressions of $\mathbf{C}_a$, $\mathbf{C}_v$ and $\mathbf{C}_d$ into equations (31d) and (31e), an additional equation can be obtained as shown below

$$\bar{\mathbf{h}}_k\mathbf{M} + \bar{\mathbf{h}}_{k-1}\mathbf{E} + \bar{\mathbf{h}}_{k-2}\mathbf{K} = \mathbf{0}, \quad k \geqslant 3. \tag{34}$$

An over-determined linear matrix equation for the estimation of structural system matrices is now written as

$$\begin{bmatrix} \bar{\mathbf{h}}_0 & 0 & 0 \\ \bar{\mathbf{h}}_1 & \bar{\mathbf{h}}_0 & 0 \\ \bar{\mathbf{h}}_2 & \bar{\mathbf{h}}_1 & \bar{\mathbf{h}}_0 \\ \bar{\mathbf{h}}_3 & \bar{\mathbf{h}}_2 & \bar{\mathbf{h}}_1 \\ & \bar{\mathbf{h}}_3 & \bar{\mathbf{h}}_2 \\ & & \bar{\mathbf{h}}_3 \\ & \vdots & \end{bmatrix} \begin{bmatrix} \mathbf{M} \\ \mathbf{E} \\ \mathbf{K} \end{bmatrix} = \begin{bmatrix} \mathbf{C}_a \\ \mathbf{C}_v \\ \mathbf{C}_d \\ 0 \\ 0 \\ 0 \\ \vdots \end{bmatrix} \tag{35}$$

or in matrix form

$$\tilde{\mathbf{G}}\tilde{\mathbf{X}} = \tilde{\mathbf{Y}}. \tag{36}$$

The matrix $\tilde{\mathbf{G}}$ is a block Toeplitz matrix with non-symmetrical block entities, and each block entity along each diagonal direction is the same. The block entities, i.e., the Markov parameters, basically are symmetrical matrices for displacement, velocity or acceleration measurements only. It is not symmetrical in the case of the mixed measurements. The row dimension of matrix $\tilde{\mathbf{G}}$ may be infinite; hence it is inconvenient for the computation of

structural system matrices using equation (36). A submatrix of $\tilde{\mathbf{G}}$, namely $\tilde{\mathbf{G}}_k \in R^{n(k+1)\times 3n}$ is used in this paper to solve the over-determined system

$$\tilde{\mathbf{G}}_k = \begin{bmatrix} \bar{\mathbf{h}}_0 & 0 & 0 \\ \bar{\mathbf{h}}_1 & \bar{\mathbf{h}}_0 & 0 \\ \bar{\mathbf{h}}_2 & \bar{\mathbf{h}}_1 & \bar{\mathbf{h}}_0 \\ \bar{\mathbf{h}}_3 & \bar{\mathbf{h}}_2 & \bar{\mathbf{h}}_1 \\ \vdots & \vdots & \vdots \\ \bar{\mathbf{h}}_k & \bar{\mathbf{h}}_{k-1} & \bar{\mathbf{h}}_{k-2} \end{bmatrix}. \tag{37}$$

The subscript of $\tilde{\mathbf{G}}_k$ indicates the subscript of the last entity of the first block column in the block matrix $\tilde{\mathbf{G}}_k$. The structural system matrices are computed by making use of the Moore–Penrose pseudo-inverse of $\tilde{\mathbf{G}}_k$ as

$$\tilde{\mathbf{X}} = \begin{bmatrix} \mathbf{M} \\ \mathbf{E} \\ \mathbf{K} \end{bmatrix} = \tilde{\mathbf{G}}_k^{+}\,\tilde{\mathbf{Y}}_k, \tag{38}$$

where $\tilde{\mathbf{Y}}_k$ is a submatrix of $\tilde{\mathbf{Y}}$ that has the same block row number as $\tilde{\mathbf{G}}_k$. The fundamental rule for selecting an adequate k in the matrix $\tilde{\mathbf{G}}_k$ is to transform the matrix into a full rank matrix. In general, $k \geqslant 4$ is suggested for estimating the structural system matrices using equation (38).

In the case of only one type of measurement, the solution of structural system matrices can be found from equations (30a)–(31d) as follows:

$$\hat{\mathbf{M}} = \bar{\mathbf{h}}_j^{-1}, \qquad \hat{\mathbf{E}} = -\bar{\mathbf{h}}_j^{-1}\bar{\mathbf{h}}_{j+1}\bar{\mathbf{h}}_j^{-1}, \qquad \hat{\mathbf{K}} = \bar{\mathbf{h}}_j^{-1}(\bar{\mathbf{h}}_{j+1}\bar{\mathbf{h}}_j^{-1}\bar{\mathbf{h}}_{j+1} - \bar{\mathbf{h}}_{j+2})\bar{\mathbf{h}}_j^{-1}, \tag{39a–c}$$

where $j = 0$ for acceleration, $j = 1$ for velocity, and $j = 2$ for displacement only.

The estimation of structural system matrices from displacement-based Markov parameters reported in reference [17] is a special case of our results, i.e., the case of $j = 2$. Once the continuous-time Markov parameters have been estimated from an equivalent state-space system, the structural system matrices can be estimated from adequate expressions depending on the types of sensors used in the measurement.

5. NUMERICAL EXAMPLES

In order to illustrate the availability of this proposed method, a lumped mass model with three d.o.f. was selected as a study case. The parameters of this model shown in Figure 1 are $m_1 = 1$, $m_2 = 2$, $m_3 = 3$, $c_1 = c_4 = c_5 = 0{\cdot}1$, $c_2 = c_3 = 0{\cdot}2$, $k_1 = 10$, $k_2 = 20$ and $k_3 = 30$. The excitation forces that acted on the 3-d.o.f. are Gaussian white-noise sequences with zero mean and unit variance. A fourth order Runge–Kutta method was employed to calculate the displacement, velocity and acceleration response at m_1, m_2 and m_3 respectively. The sampling rate of measurement was selected as 5 Hz, and 1024 data points of displacement, velocity and acceleration responses were picked. The time histories of response of different sensors at different positions are shwon in Figure 2. The magnitude and change rate of the time histories of the measured displacement, velocity and acceleration are apparently different. In order to show the effects of noise on the accuracy level of the identified system matrices of structures and the associated modal parameters, a zero mean white noise was

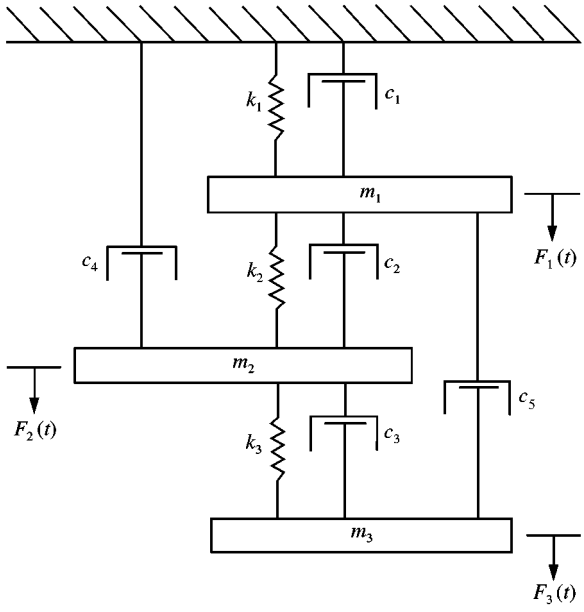

Figure 1. Three-d.o.f. lumped mass model.

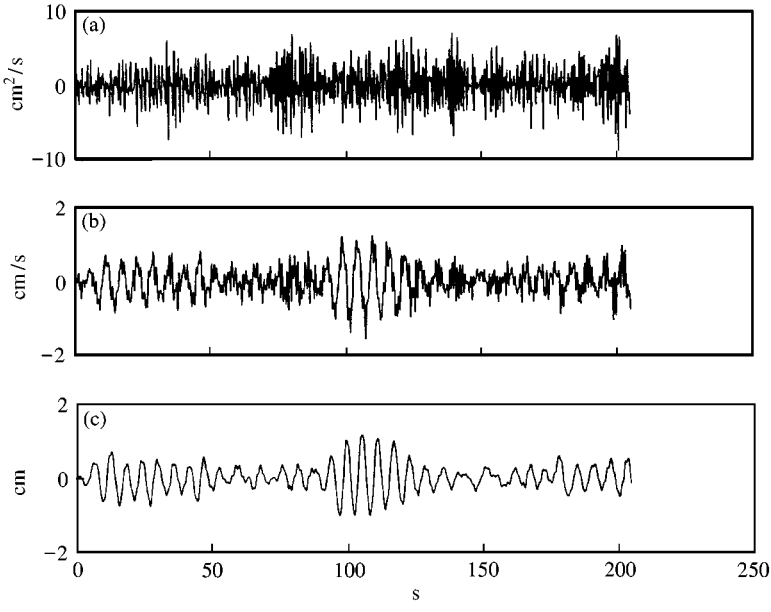

Figure 2. Time history of responses of 3-d.o.f. model to white-noise excitation. (a) acceleration at m_1; (b) velocity at m_2; (c) displacement at m_3.

added to the original noise-free response data to simulate the measurement noise of real world. Five levels of contaminated measurement noise with the r.m.s. value equal to 1, 3, 5, 10 and 20% of the r.m.s. of noise-free response data were taken into consideration. One hundred runs of Monte Carlo simulation for each noise level were performed to study the

statistical characteristics of the accuracy level of the identified system matrices and modal parameters. The relative error of the identified structure parameters is defined as

$$\textit{Relative error of } \bar{Q} = \frac{\|Q - \bar{Q}\|_2}{\|Q\|_2} \times 100\%, \tag{40}$$

where Q represents the original structure parameters, such as structural system matrices or modal parameters; $\bar{Q}$ is the identified Q, and $\|Q\|_2$ is the second norm of Q. The relative error of the identified structural system matrices in the case of 1, 5 and 20% noise levels for the 100 runs are shown in Figures 3–5. In these figures, the horizontal line in each noise level indicates the average relative error of the 100 runs. Because of the random nature of

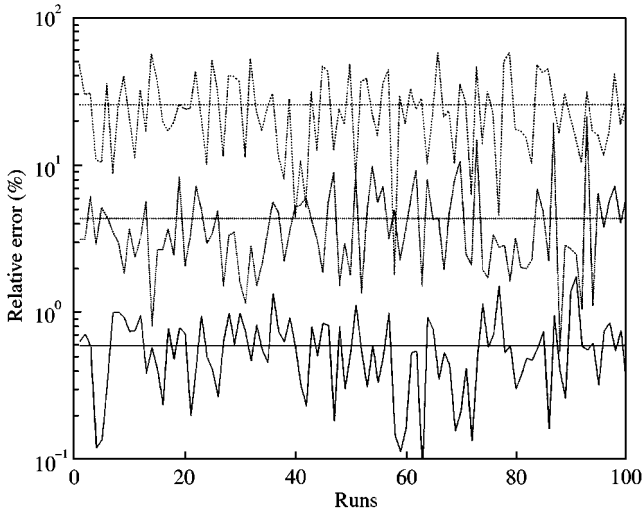

Figure 3. Relative error of identified mass matrix for different noise levels. -, 1%; --, 5%; ··, 20%.

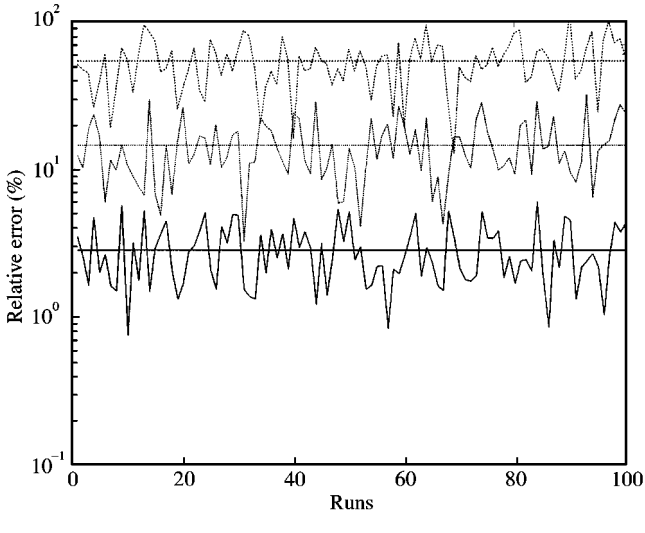

Figure 4. Relative error of identified damping matrix for different noise levels. -, 1%; --, 5%; ··, 20%

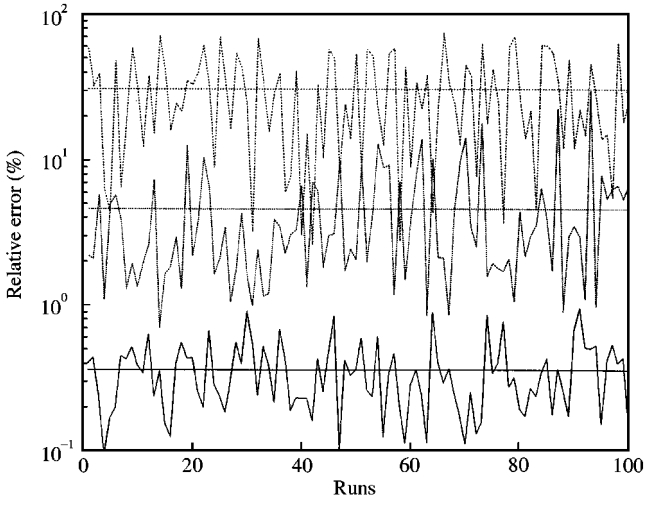

Figure 5. Relative error of identified stiffness for different noise levels. -, 1%; --, 5%; ··, 20%.

TABLE 1

Average and standard deviation of the relative errors for the identified mass, damping and stiffness matrices at different noise levels

Noise level	1%		3%		5%		10%		20%	
	Ave.	Std.	Ave.	Std.	Ave.	Std.	Ave.	Std.	Ave.	Std.
Mass	0·59	0·32	2·17	1·43	4·34	3·36	11·12	7·59	25·63	13·83
Damp.	2·82	1·28	8·12	4·25	14·44	6·60	30·28	14·50	54·28	19·68
Stiff.	0·36	0·20	1·86	1·72	4·62	4·73	13·00	11·13	30·96	20·18

measurement noise, the relative errors of the identified structural system matrices for different noise levels fluctuate around their average relative error. Table 1 shows the average and the standard deviation of relative errors of identified structural system matrices for all noise levels. The average and the standard deviations of relative errors of the identified structural system matrices are generally increased with the increment of noise level. The relative error for the identified damping matrix is higher than those of the identified mass and stiffness matrices at all noise levels. This also reflects a fact that the damping property is more difficult to be identified precisely than the mass and stiffness properties. The error seems to be reasonable in the case of low noise level (1 and 3%), but it has a rather large value of error at high noise level. For example, the average and standard deviation of the relative error of identified damping matrix in the case of 20% noise level are 54·28 and 19·68% respectively.

Table 2 shows the true modal parameters of the 3-d.o.f. lumped model. The mean values and standard deviations of the identified natural frequencies and damping ratio from the 100 runs are shown in Tables 3 and 4. Figure 6 shows the distribution of average relative errors of identified modal parameters from the 100 runs versus the different noise levels. The results show that the average relative errors of the modal parameters are much lower than that of system matrices. The relative errors are large at high noise level (20%),

TABLE 2

True natural frequencies, damping ratios and normalized mode shapes of 3-d.o.f. lumped mass model

	Mode 1	Mode 2	Mode 3
Natural frequency (Hz)	0·1699	0·7120	1·0537
Damping ratio (%)	1·7626	3·4783	3·7849
Mode shape	0·2761 0·3983 0·4496	0·6667 0·3333 − 0·3333	0·6924 − 0·4798 0·1417

TABLE 3

The average and standard deviation of identified natural frequencies at different noise levels for 3-d.o.f. lumped mass model

Mode	1%		3%		5%		10%		20%	
	Ave.	Std.	Ave.	Std.	Ave.	Std.	Ave.	Std.	Ave.	Std.
1	0·1699	5·4e − 5	0·1699	1·8e − 4	0·1699	2·9e − 4	0·1699	5·2e − 4	0·1699	1·2e − 3
2	0·7120	1·31e − 4	0·7120	3·96e − 4	0·7121	7·8e − 4	0·7120	1·5e − 3	0·7118	3·1e − 3
3	1·0537	9·3e − 5	1·0537	2·9e − 4	1·0538	5·0e − 4	1·0536	9·4e − 4	1·0536	1·8e − 3

TABLE 4

The average and standard deviation of identified damping ratios at different noise levels for 3-d.o.f. lumped mass model

Mode	1%		3%		5%		10%		20%	
	Ave.	Std.	Ave.	Std.	Ave.	Std.	Ave.	Std.	Ave.	Std.
1	1·7580	3·8e − 2	1·7475	1·1e − 1	1·7750	1·7e − 1	1·7314	3·7e − 1	1·8886	8·4e − 1
2	3·4779	3·6e − 3	3·4763	1·1e − 2	3·4841	1·7e − 2	3·4771	3·7e − 2	3·4926	8·0e − 2
3	3·7848	3·1e − 3	3·7843	9·1e − 3	3·7845	1·7e − 2	3·7869	3·1e − 2	3·7978	6·1e − 2

but it can be improved by increasing the number of data points. Figure 7 shows the relative error of the identified natural frequency and damping ratio of the first mode in the case of 20% noise level versus the number of data points. The trend of relative error is roughly decreasing with the increment of number of data points. Figure 8 shows the normalized mode shape for the true shape and the identified modes for 3, 10 and 20% noise levels. The results show that the identified mode shapes are in good agreement with the true one. The correlation between the identified mode shape and the true one can be evaluated by modal assurance criterion (MAC) [27]. A value of MAC close to 1·0 indicates that the two mode shapes are approximately parallel. Figure 9 shows the distribution of MAC values in the 100 runs for 1, 5 and 20% noise levels. The MAC values in all three modes are all close to 1 except in the case of 20% noise level.

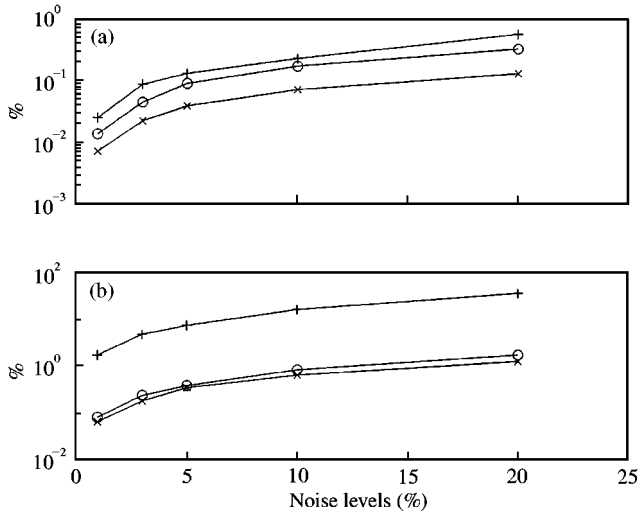

Figure 6. Average relative errors of identified modal parameters at different noise levels. (a) natural frequencies; (b) damping ratios. +, first mode; ○, second mode; ×, third mode.

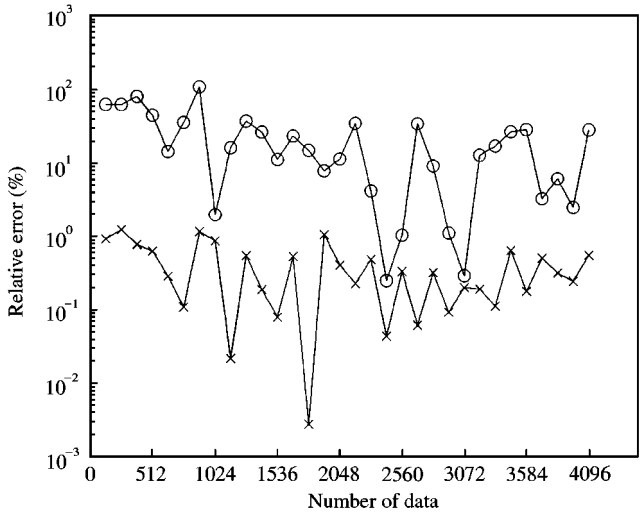

Figure 7. Relative errors of identified modal parameters versus the number of data points (20% noise level, first mode). ×, for natural frequency, ○, for damping ratio.

6. CONCLUSION

This work presented a method to extract the system matrices of structures from a continuous-time state-space system that is identified from the combined measurement of displacement, velocity and acceleration responses, as well as the input excitations. By employing the invariant property of Markov parameters in the continuous-time, the relationship between the Markov parameters, the structural system matrices and the output influence matrices for displacement, velocity and acceleration has been derived. The presented method is also valid when only the displacement, velocity or acceleration is

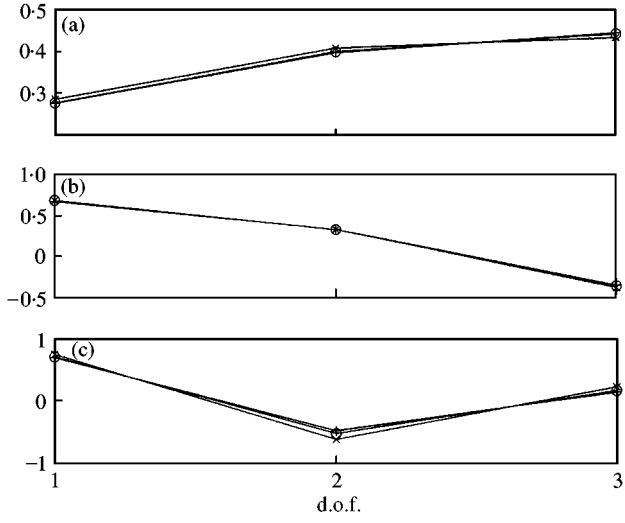

Figure 8. The average of normalized mode shapes at different noise levels. ——, 0%; +, 3%; ○, 10%; ×, 20%. (a) first mode, (b) second mode, (c) third mode.

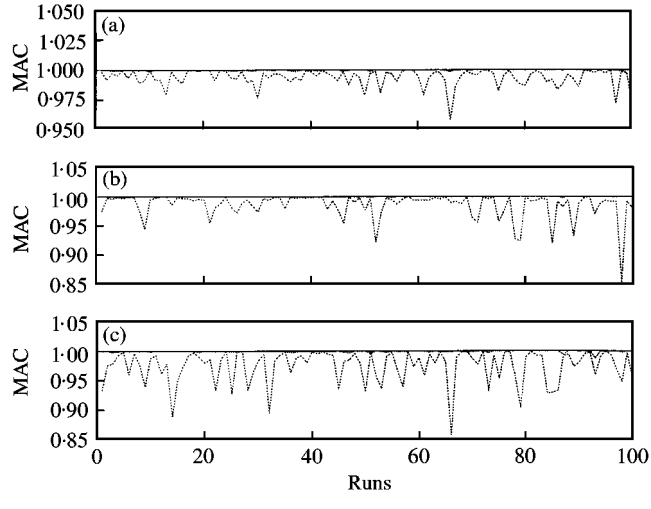

Figure 9. The distribution of MAC value versus the 100 runs at different noise levels. (a) first mode; (b) second mode; (c) third mode. -, 1%; --, 5%, ··, 20%.

measured. In this work, an efficient method, which combines the ARX model with the ERA, is employed for identifying the equivalent state-space system. The results of the numerical example show that the relative errors in the identification of natural frequencies and damping ratios are considerably lower than the relative errors in the identified structural system matrices. The numerical results of Monte Carlo simulations show that the presented method provides feasible and acceptable results.

ACKNOWLEDGMENTS

The authors gratefully acknowledge the financial support of the National Science Council, Republic of China, under project numbers NSC 86-2611-E-002-006 and NSC 87-2611-E-002-049.

REFERENCES

1. C. S. Li and W. J. Ko 1988 *Royal Institution of Naval Architects* **130**, 315–327. On the application of the time series in structural failure detection and monitoring for offshore applications.
2. P. Stoica 1990 *Signal Processing* **19**, 301–310. Performance evaluation of some methods for off-line detection of changes in autoregressive signals.
3. T. W. Lim 1991 *American Institute of Aeronautics and Astronautics Journal* **29**, 2271–2274. Structural damage detection using modal test data.
4. M. Baruch 1982 *American Institute of Aeronautics and Astronautics Journal* **20**, 1623–1626. Optimal correction of mass and stiffness matrices using measured modes.
5. A. Berman and E. J. Nagy 1983 *American Institute of Aeronautics and Astronautics Journal* **21**, 1168–1173. Improvement of a large analytical model using test data.
6. F. S. Wei 1990 *American Institute of Aeronautics and Astronautics Journal* **28**, 175–177. Analytical dynamic model improvement using vibration test data.
7. P. Ladeveze, D. Nedjar and M. Reynier 1994 *American Institute of Aeronautics and Astronautics Journal* **32**, 1485–1490. Updating of finite element models using vibration tests.
8. D. J. Ewins 1984 *Modal Testing Theory and Practice*. London: Research Studies Press Ltd.
9. M. Baruch 1997 *American Institute of Aeronautics and Astronautics Journal* **35**, 1797–1798. Modal data are insufficient for identification of both mass and stiffness matrices.
10. S. Y. Chen, M. S. Ju and Y. G. Tsuei 1996 *American Society of Mechanical Engineers Journal of Vibration and Acoustics* **118**, 78–82. Estimation of mass, stiffness and damping matrices from frequency response functions.
11. S. Y. Chen and Y. G. Tsuei 1995 *American Institute of Aeronautics and Astronautics Journal* **33**, 2199–2204. Estimation of system matrices by dynamic condensation and application to structural modification.
12. K. F. Alvin, L. D. Peterson and K. C. Park 1995 *American Institute of Aeronautics and Astronautics Journal* **33**, 128–135. Methods for determining minimum-order mass and stiffness matrices from modal test data.
13. P. Yuan, Z. Wu and X. Ma 1998 *Earth Engineering and Structural Dynamics* **27**, 415–427. Estimated mass and stiffness matrices of shear building from modal test data.
14. M. Okuma, Q. Shi and T. Oho 1999 *Journal of Sound and Vibration* **219**, 5–22. Development of the experimental spatial matrices identification method (Theory and basic verification with a frame structure.)
15. J. N. Juang and R. S. Pappa 1985 *Journal of Guidance, Control, and Dynamics* **8**, 620–627. An eigensystem realization algorithm for modal parameters identification and model reduction.
16. J. N. Juang and R. S. Pappa 1986 *Journal of Guidance, Control, and Dynamics* **9**, 294–303. Effect of noise on modal parameters identified by the eigensystem realization algorithm.
17. C. D. Yang and F. B. Yeh 1990 *Journal of Guidance, Control and Dynamics* **13**, 1051–1059. Identification, reduction, and refinement of model parameters by the eigensystem realization algorithm.
18. M. T. A. Chaudhary, M. Abe, Y. Fujino and J. Yoshida 2000 *Journal of Structural Engineering* **126**, 1187–1195. System identification of two base-isolated bridges using seismic records.
19. C. F. Hung, W. J. Ko and C. H. Tai 2000 *The First International Conference on Structural Stability and Dynamics*, Taipei, Taiwan, December 7–9. Identification of modal parameters from the combined DVA measured data under unknown input force.
20. J. N. Juang 1994 *Applied System Identification*. Englewood Cliffs, NJ: Prentice-Hall.
21. W. J. Rugh 1996 *Linear System Theory*. Englewood Cliffs, NJ: Prentice-Hall; second edition.
22. T. Soderstrom 1989 *System Identification*. London: Prentice-Hall.
23. L. Liung 1987 *System Identification: Theory for the User*. Englewood Cliffs, NJ: Prentice-Hall .
24. H. C. Lee, M. H. Hsaio, J. K. Huang and C. W. Chen 1996 *Journal of Vibration and Acoustics* **118**, 169–175. Identification of stochastic system and controller via projection filters.
25. C. W. Chen, J. K. Huang, M. Phan and J. N. Juang 1992 *Journal of Guide, Control and Dynamics* **15**, 88–95. Integrated system identification and modal state estimation for control of large flexible space structures.
26. J. N. Juang, M. Phan, L. G. Horta and R. W. Longman 1993 *Journal of Guide, Control and Dynamics* **16**, 320–329. Identification of observer/Kalman filter Markov parameters: theory and experiment.
27. R. J. Allemang and D. L. Brown 1982 1*st International Modal Analysis Conference, Orlando, FL*, 110–116. A correlation coefficient for modal vector analysis.